Journal of Geology & Geosciences
ISSN: 2381-8719

Chun-Ming et al., J Geol Geosci 2014, 3:3
DOI: 10.4172/2329-6755.1000153

Research Article Open Access

# Re-Os Dating of Molybdenites from the Daheishan Mo Deposit in the Eastern Central Asian Orogenic Belt, NE China, and its Geological Significance

**Han Chun-Ming*[1], Wu Fu-Yuan[1], Xiao Wen-Jiao[1], Zhao Guo-Chun[2], Ao Song-Jian[1], Zhang Ji-Een[1], Wan Bo[1], Qu Wen-Jun[3] and Du An-Dao[3]**

[1]*Key Laboratory of Mineral Resources, Institute of Geology and Geophysics, Chinese Academy of Sciences, Beijing 100029, China*
[2]*Department of Earth Sciences, The University of Hong Kong, Pokfulam Road, Hong Kong, China*
[3]*National Research Center of Geoanalysis, Beijing, 100037, China*

**Abstract**

The Daheishan Mo deposit is located in the eastern part of the Central Asian Orogenic Belt NE China. Rhenium and osmium isotopes in molybdenites from the Daheishan porphyry Mo deposit have been used to determine the age of mineralization. Molybdenite was analyzed mainly from granodiorite porphyry, which is characterized by moderate to strong silicification. Rhenium concentrations in molybdenite samples are between 17 and 30 μg/g. Analysis of seven molybdenite samples yields an isochron age of 168.0 ± 4.4 Ma (2σ). Based on the geological history and spatial-temporal distribution of the granitoids, it is proposed that the Mo deposits in the eastern China were related to the subduction of the Paleo-Pacific plate during Jurassic time.

**Keywords:** Re-Os study; Mo deposit; Daheishan; The Central Asian Orogenic Belt

## Introduction

The Mesozoic tectonics of NE China was characterized by the orogenic events of the Paleo-Asian domain superimposed by the subduction-related orogenesis of the Pacific domain, generating widespread Mesozoic volcanic and granitic rocks together with important mineral deposits of Cu, Mo, Fe, Ni and Au in China [1-5] (Table 1). However, when these geodynamic domains were transferred is an open question [6] and the direct connection between geodynamic processes and the mineral deposits is not clear [1,4]. Many researchers have studied these orogenic events and volcanic and granitic rocks but these enigmatic points remain to be understood. It is obvious that the tectonic setting and formation age of some representative ore deposits are important in addressing these problems.

In the present study, we carried out Re-Os dating of molybdenum ores from the Daheishan deposit, the largest and economically most important Mo deposit in the CAOB in order to constrain the timing of mineralization. In addition, we also discuss the geodynamic environments and processes that controlled the ore formation. An understanding of these mineralizing processes and geodynamic environments has important implications for the Mo exploration in the eastern part of the CAOB.

## Geological Setting

The eastern Central Asian Orogenic Belt (CAOB) contains a number of Paleozoic and Mesozoic terranes that amalgamated between the Siberian and the North China Cratons, and underwent complex tectonic evolution [2,3,7]. The NE China is divided into four tectonic Blocks (Erguna, Xing'an, Songliao and Jiamusi Blocks), which are separated by the regional-scale Tayuan-Xiguitu, Hegenshan-Heihe and Mudanjiang faults, respectively [4]. The Songliao Block joined the Xing'an block along the Hegenshan-Nenjiang Fault in the Late Paleozoic and it was accreted to the North China Craton along the Xilamulun-Changchun belt, during the Late Permian and early Triassic and marked the final closure the Paleo-Asian ocean [8,9] (Figure 1). During the Mesozoic, the Jamusi Block accreted to this merged block along the Mudanjiang Fault [4,10] . The studied Daheishan deposit is located in the Songnen Block (Figure 1).

In the Songliao Block, the Late Paleozoic series consists of shallow water continental shelf deposits (Figure 2; [11]). Cambrian and Ordovician limestone and argillite are overlain by Carboniferous and Permian limestone, sandstone, and shale. Eastward, the Hulan group mainly consisted of metamorphic rocks, and a mafic-ultramafic association of the Hongqiling Group [3,12]. The upper greenschist to amphibolite facies metamorphic rocks, namely biotite-garnet ± kyanite micaschists, quartzites, marbles and amphibolites enclose gabbro, diabase, serpentinite, ultramafic rocks some of which contain economic Ni-Cu concentrations [12]. On the basis of LA-ICP-MS dating of detrital zircons in the metapelites, an Early Permian age (ca. 290 Ma) is inferred for the age of the metamorphic rocks [11].

A series of faults are recognized in the Daheishan deposit. There are three groups of faults, with EW-, NNE- and NE-trending strikes. The NNE-striking faults are large-scale, and have undergone multiple stages of movement. The intersections of EW-striking faults with NNE-striking faults are favorable locations for emplacement of the granite-porphyry complexes [13]. The Toudaogou Formation is the country rock of granitoids at the Daheishan Mo deposit, and can be subdivided into two sections [3]. The lower section is mainly composed of metamorphosed intermediate-mafic to intermediate-felsic volcanics with intercalated meta-sandstone and meta-tuff. The upper section is composed of arenaceous slate, with interlayers of metamorphosed intermediate-felsic volcanics and lenses of marble. The Nanloushan Formation unconformably overlies the Toudaogou Formation and is composed of intermediate-felsic volcanic and volcanoclastic rocks. According to field relationship, contact relationships and mineralization features, the granitoids in this area can be subdivided into two episodes; Late Triassic unmineralized biotite granodiorite with minor monzogranite, and Jurassic ore-bearing granodiorite porphyry and felsitic granodiorite [3].

***Corresponding author:** Han Chun-Ming, Key Laboratory of Mineral Resources, Institute of Geology and Geophysics, Chinese Academy of Sciences, Beijing 100029, China, Tel: 86 10 6200 8004; E-mail: cm-han@mail.iggcas.ac.cn

**Received** March 01, 2013; **Accepted** March 19, 2014; **Published** March 24, 2014

**Citation:** Chun-Ming H, Fu-Yuan W, Wen-Jiao X, Guo-Chun Z, Song-Jian A, et al. (2014) Re-Os Dating of Molybdenites from the Daheishan Mo Deposit in the Eastern Central Asian Orogenic Belt, NE China, and its Geological Significance. J Geol Geosci 3: 153. doi: 10.4172/2329-6755.1000153

| Deposits | Genetic types | Economic metals | Host rocks | Intrusive rocks | Wall-rock alteration | Reserve, Grade | Orebody size | Sulfide assemblages | References |
|---|---|---|---|---|---|---|---|---|---|
| Duobaoshan (125°47′00″E 50°15′00″N) | Porphyry | Cu-Mo | Middle-Ordovi:Andesite, tuff, tuff lava, volcanic breeica | Quartz-diorite, Quartz-diorite-porphyry | Silicification, k-feldspar alteration, sericitization, chloritization, carbonization | 5071tMo Mo:0.10%; 72172t Cu Cu:0.20-0.60% | Length:225-1400m;Wideness: 25-713m; Depth:24-594m | Molybdenite, pyrite, chalcopyrite, bornite, copper glance, galena, zinc blende | [13] |
| Wudaoling (127°13′52″E 45°18′08″N) | Skarn | Mo | Upper-Permian Tuffaceous sandstone, liparite-tuff, andesite-tuff | Granite, diorite and granodiorite | Skarnization, silicification, sericitization, chloritization, carbonization, epidotization | 41584tMo Mo:0.038-0.172% | Length:50-558m; Thickness:1-99m; Depth:40-770m | Molybdenite, pyrite, Haematite, chalcopyrite, copper glance, bornite, galena, zinc blende | |
| Changgang (126°15′26″E 43°28′04″N) | Porphyry | Mo | Upper-Permian Tuff, hornstone, episandstone, limestone | Diorite, granite-porphyry | Epidotization, silicification, carbonization, chloritization | 9620tMo Mo:0.035-0.092% | Length:93-394m Thickness:0.50-13m; Depth:7000m | Dipyrite, molybdenite, pyrite, galena, zinc blende, chalcopyrite | |
| Tiegongshan | Skarn | W-Mo | Upper-Permian: Marble, limestone, | Granite, granitite, porphyritic granite | Skarnization, k-feldspar alteration, epidotization, silicification, chloritization | 5220t $WO_3$; $WO_3$:0.254%; 2198tMo; Mo:0.145%; 571tZn;Zn:4.29% | Length:260-500m ; Wideness:60-70m | Molybdenite, Scheelite, magnetite, zinc blende | |
| Qiupigou (127°11′00″E 45°38′04″N) | Porphyry | Cu-Mo | Lower-Permian: Episandstone, Marble, andesite, rhyolite | Granitite, granodiorite, porphyritic granite, Granodiorite-porphyry | Skarnization, k-feldspar alteration, silicification, greisenization | 3805tMo Mo:0.023-0.060% | Length:80-375m Thickness:2-6m; Depth:5-130m | Molybdenite, Tetrahedrite, zinc blende, chalcopyrite, pyrite, chalcocite | |
| Shirengou (128°50′30″E 42°00′00″N) | Porphyry | Mo | Porphyritic granodiorite, granodiorite | Aplite granite | Skarnization, epidotization, silicification, chloritization | 3517tMo Mo:0.102-0.113% | Length:10-192m Thickness:1.9-13.1m; Depth:5-130m | Pyrite, Molybdenite, zinc blende, galena, chalcopyrite | |
| Daheishan (126°16′00″E 3°29′00″N) | Porphyry | Mo | Biotite granodiorite porphyry | Biotite granodiorite porphyry | Sericitization, silicification, carbonatization, chloritization, epidotization and potassic alteration | 1.08MtMo Mo:0.01-0.12% | Length:1700m Wideness:1700m; Depth:500m | molybdenite , Pyrite, chalcopyrite, zinc blende, galena, magnetite, kroeberite, chalcomiclite. | |

**Table 1:** Summary of geological and mineralogical features of molybdenum and copper deposits in the Yanshan-Liaoning metallogenic belt.

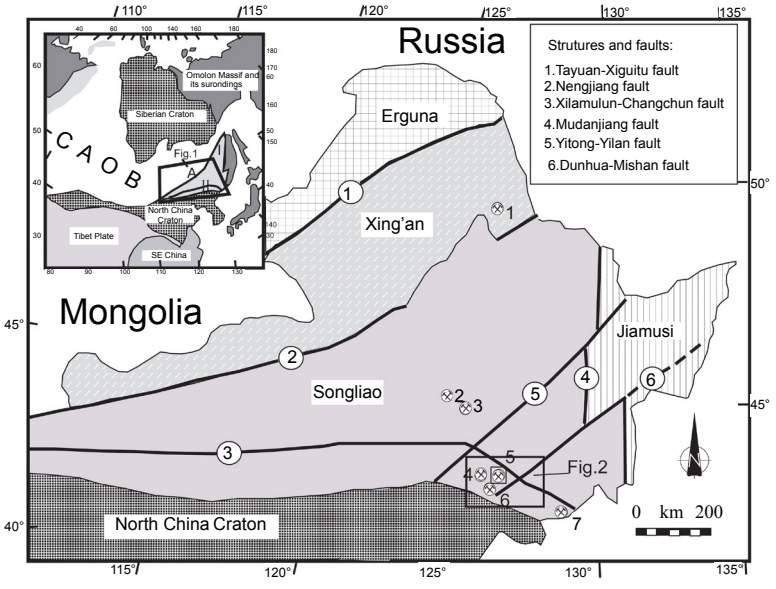


**Figure 1:** The map showing the distribution of the major molybdenum deposits in the east Central Asian Orogenic Belt [3]. 1=Duobaoshan; 2=Qiupigou; 3=Wudaoling; 4=Changgang; 5=Daheishan; 6=Tiegongshan; 7=Shirengou.

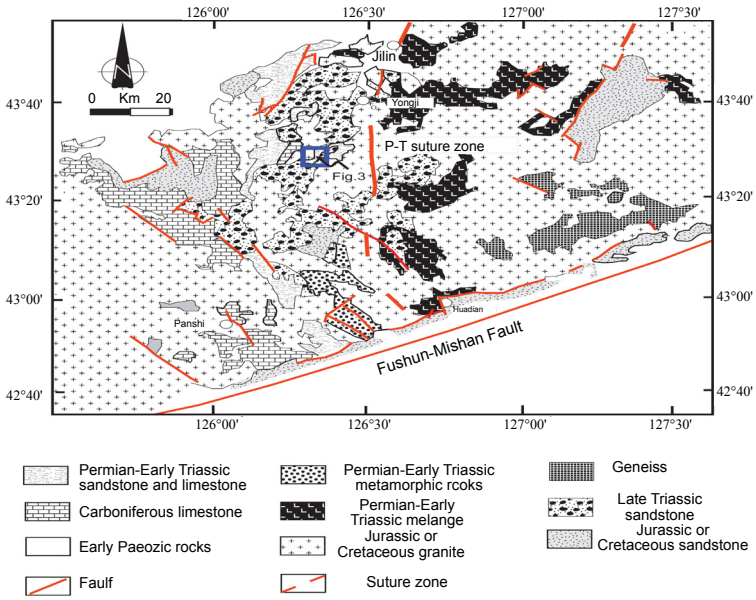


**Figure 2:** Geological map of the central Jilin Province [11]. Inset shows location of the area with respect to the regional geological setting of China and Russia (outline shows location of studied area in NE China). (I) Hegenshan-Hehei suture zone, (II) Solonker-Xra Moron-Changchun suture zone

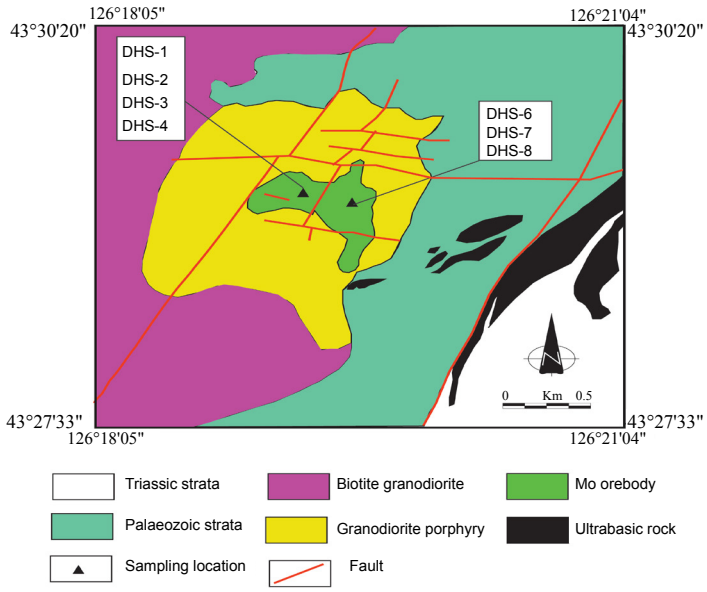


**Figure 3:** Geological map of the Daheishan Mo deposit (modified after [4]).

## Daheishan Mo Deposit

The Daheishan deposit is characterized by a total Mo metal reserve of 1.09 Mt and average Mo concentrations of 0.06% [13]. It was discovered in 1952 and exploited during the period 1954–1983 by the No.2 Institute Tonghua Geological Survey of Jilin Province [13]; production from the currently operating mine began in 1985. The Daheishan intrusion is composed of biotite granodiorite and granodioritic porphyry, with minor granite porphyry, and the Mo ore body is hosted by the biotite granodiorite and granodioritic porphyry. The biotite granodiorite is fine-medium grained with a massive structure, with a mineral assemblage represented by plagioclase (50%-60%), quartz (20%-30%), K-feldspar (5%-10%), biotite (5%-10%) and minor amphibole (2%-5%). The plagioclase is generally altered to sericite, with relics showing polysynthetic twins and zonal structure. Perthitic texture in K-feldspar can be observed occasionally. Apatite, magnetite and zircon form the accessory mineral phases [3]. The granodioritic porphyry is characterized by a massive and porphyritic, with micro-hypidiomorphic to allotriomorphic granular-texture, locally with a felsitic matrix. The phenocrysts are euhedral to subhedral plagioclase and euhedral quartz, and plagioclase phenocrysts are generally altered to sericites. The matrix is made up of plagioclase, quartz, biotite and minor K-feldspar. Zircon, magnetite and apatite are the accessory mineral phases. The granodioritic porphyry yields a zircon SHRIMP U-Pb age of 170 ± 3Ma [3]. The orebody has a circular shape, with a maximum length and a

width of up to 1700 m, and has a surface outcrop of ~2.3 km$^2$ (Figure 3). There is no a distinct boundary between orebody and country rocks. The ores are characterized by euhedral and subhedra textures, and veinlet-disseminated, veinlets, massive and disseminated sulphides (Figure 4). Principal metallic minerals are molybdenite and pyrite, with minor amounts of chalcopyrite, sphalerite, galena, magnetite and kroeberite. The gangue minerals include mainly plagioclase and quartz, with lesser amounts of biotite, sericite, calcite, K-feldspar, chlorite and epidote. Wall rocks are variably altered to sericite, silica, carbonate, chlorite, epidote and K-feldspar. So far there is no direct information on the age of the ore formation. Based on crosscutting relationships

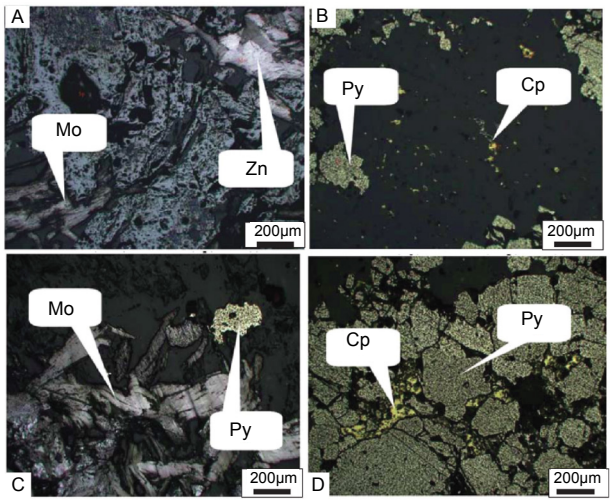


**Figure 4:** Photographs showing mineralization at the Daheishan Mo deposit. (A) Disseminated molybdenite and massive sphalerite. (B) Disseminated pyrite and chalcopyrite. (c). Molybdenite veins and disseminated pyrite. (d) Late chalcopyrite veins and disseminated pyrite.

| Minerals | Stage 1 | Stage 2 | Stage 3 | Stage 4 | Stage 5 |
|---|---|---|---|---|---|
| Magnetite | | | | | |
| Gregorite | | | | | |
| Pyrite | | | | | |
| Molybdenite | | | | | |
| Chalcopyrite | | | | | |
| Kroeberite | | | | | |
| Sphalerite | | | | | |
| K-feldspar | | | | | |
| Muscovite | | | | | |
| Quartz | | | | | |
| Chlorite | | | | | |
| Epidote | | | | | |
| Calcite | | | | | |
| Liminite | | | | | |
| Malachite | | | | | |
| Barite | | | | | |
| Molybdic ocher | | | | | |

**Figure 5:** Paragenesis sequences of minerals of the Daheishan Mo deposit (modified after [13]).

of minerals and mineral assemblages, alteration and mineralization in the Daheishan ore body can be divided into five stages [13] (Figure 5). Stage 1 is characterized by chlorite, epidote and K-feldspar alteration, with pyrite + molybdenite + magnetite as the representative ore mineral assemblage. Stage 2 is characterized mainly by sericitan and silica alteration, associated with disseminations of magnetic pyrite + molybdenite + pyrite + chalcopyrite ore minerals. Stage 3 is the main mineralization stage and characterized by silica alteration, represented by the formation of veins containing quartz + pyrite + molybdenite + chalcopyrite + sphalerite + galena. Stage 4 is characterized by carbonate alteration, and a carbonate (calcite) + barite + minor sulfides assemblage. Stage 5 is marked by supergene oxidation, resulting in the formation of some secondary minerals (e.g. limonite).

## Sampling and Analytical Methods

We selected 7 samples from the Daheishan Mo deposit for Re-Os dating (Figure 3), all of which were collected from fresh open-pit mining faces. Sampling locations are show in Figure 3. Re-Os isotopic analyses were performed at the National Research Center of Geoanalysis, Chinese Academy of Geosciences. The details of the chemical procedure have been described by [14-19]. They are briefly described as follows. The Carius tube (a thick-walled borosilicate glass ampoule) digestion technique was used. The weighed sample was loaded in a Carius tube through a long thin-neck funnel. The mixed $^{190}$Os and $^{185}$Re spike solution and 2 ml of 10 N HCl and 6 ml of 16 N $HNO_3$ were added while the bottom part of the tube was frozen at -80 to -50°C in an ethanol-liquid nitrogen slush; the top was sealed using an oxygen-propane torch. The tube was then placed in a stainless-steel jacket and heated for 10 h at 230°C. Upon cooling, the bottom part of the tube was kept frozen, the neck of the tube was broken, and the contents of the tube were poured into a distillation flask and the residue was washed out with 40 ml of water.

Separation of osmium by distillation and separation of rhenium by extraction was performed based on the analytical method from [14,15]. A TJA PQ-EXCELL ICP-MS was used for the determination of the Re and Os isotope ratio.

Average blanks for the total Carius tube procedure were ca. 10 pg Re and ca. 1 pg Os. The analytical reliability was tested by repeated analyses of molybdenite standard HLP-5 from a carbonatite vein-type molybdenum-lead deposit in the Jinduicheng-Huanglongpu area of Shanxi Province, China. Fifteen samples were analyzed over a period of 5 months. The uncertainty in each individual age determination was about 0.35% including the uncertainty of the decay constant of $^{187}$Re, uncertainty in isotope ratio measurement, and spike calibrations. The average Re-Os age for HLP-5 is 221.3 ± 0.3 Ma (95% confidence limit, [17] Stein et al. 1997). The average Re concentration was 283.71 ± 1.54 μg/g. The average Os concentration was 657.95 ± 4.74 ng/g.

## Results

Results of molybdenite Re-Os dating are listed in Table 2. The concentrations of Re and $^{187}$Os range from 17 to 30 ng/g and 30 to 53 ng/g, respectively. Seven samples give Re–Os model ages of 167 to 169Ma and a weighted mean age of (168.32 ± 0.88Ma) Ma (Table 2). The data, processed using the ISOPLOT/Ex program [20], yielded an isochron age of (168.0 ± 4.4) Ma and with MSWD=0.65 (Figure 6).

## Discussion

### Re concentrations and possible source

Based on the published Re content in molybdenite from different

| No. Samples | Weight(g) | Re (μg/g) | | $^{187}$Re (μg/g) | | $^{187}$Os (ng/g) | | Model age | |
|---|---|---|---|---|---|---|---|---|---|
| | | Measured | 2σ | Measured | 2σ | Measured | 2σ | Measured | 2σ |
| DHS-1 | 0.05065 | 19.04 | 0.14 | 11.97 | 0.09 | 33.69 | 0.26 | 168.7 | 2.3 |
| DHS-2 | 0.05361 | 24.91 | 0.20 | 15.66 | 0.12 | 44.24 | 0.35 | 169.4 | 2.3 |
| DHS-3 | 0.05054 | 19.06 | 0.17 | 11.98 | 0.11 | 33.55 | 0.28 | 167.8 | 2.5 |
| DHS-4 | 0.05093 | 18.46 | 0.15 | 11.60 | 0.10 | 32.63 | 0.30 | 168.6 | 2.5 |
| DHS-6 | 0.05078 | 17.28 | 0.13 | 10.86 | 0.08 | 30.53 | 0.27 | 168.6 | 2.4 |
| DHS-7 | 0.05203 | 20.80 | 0.15 | 13.07 | 0.10 | 36.50 | 0.29 | 167.4 | 2.3 |
| DHS-8 | 0.05079 | 29.89 | 0.24 | 18.79 | 0.15 | 52.58 | 0.42 | 167.8 | 2.4 |

**Table 2:** Re-Os isotopic data for molybdenite from the Daheishan Mo deposit, eastern China.
Decay constant: λ ($^{187}$Re)=1.666×10$^{-11}$/year [51]. The uncertainty in each individual age determination was about 1.02%, which degree of confidence is 95%.

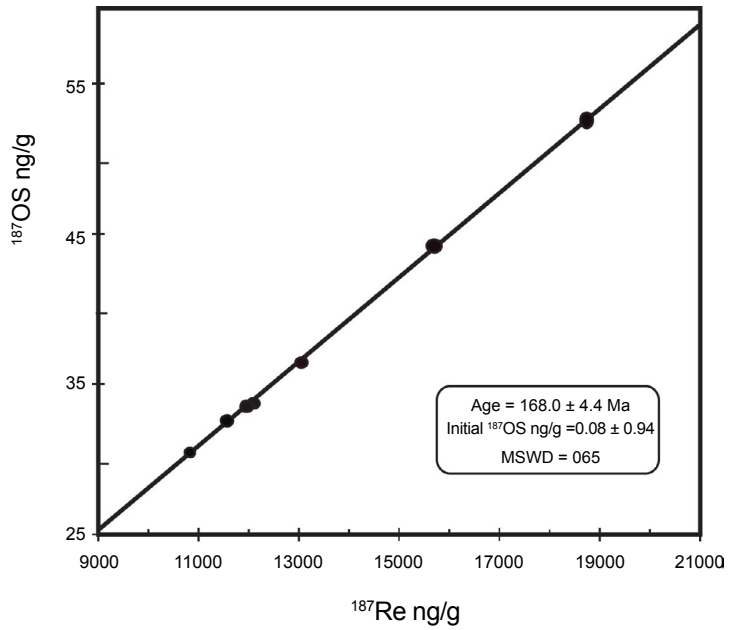


**Figure 6:** Re–Os isochron plot for molybdenite samples from the Daheishan Mo deposit.

types of endogenic Mo deposits in China, Mao et al. suggested that the rhenium contents in molybdenite decrease from a mantle source via mixtures between mantle and crust to crust [21]. This interpretation has also been favored by other researchers [22,23].

Re-Os isotope analyses indicate that the Re content in molybdenite from the Daheishan Mo deposit ranges from 18.46 to 29.89 ppm, with an average of 21.35ppm, suggesting that both mantle and crust were involved as source materials for Mo deposit [21,24,25]. This interpretation is supported by S isotopic data of sulfides from the Daheishan Mo deposit. Their $\delta^{34}S$ values vary from 1.4‰ to 2.2‰ [13], showing variable mixing the mantle-derived and crust [26]. Therefore, the $\delta^{34}S$ values also shed light on the ores from the deposit originated from variable mixtures of mantle and crust [21].

## Metallogenic geodynamic setting

Metal deposits in the eastern Central Asian Orogenic Belt (CAOB) are mainly distributed in the southern part. Based on the published ages of these deposits, two narrow intervals can be recognized: ~190Ma to 160Ma and ~150Ma to 110Ma [27-29] (Figure 7). The former may be related to the transition period from the Paleo-Asian to Pacific domains, while the latter could be mainly a result of the subduction of the Pacific plate.

During the Mesozoic, the eastern CAOB was affected by the widespread emplacement of volcanic and granitic rocks [30-32]. Recent studies suggest that the Mesozoic granites, along with a their late Paleozoic counterparts, represent significant juvenile crust addition, since these granites show positive $\varepsilon_{Nd(t)}$ values and young Nd model ages [33,34]. Late Mesozoic volcanic rocks cover ~100,000 km$^2$ with an NE–NNE trend in the eastern CAOB, with cumulative thickness of the successions up to ca. 4-5 km [35]. The lavas include a wide spectrum of rock types, including basalts, basaltic andesite, trachyte and rhyolite with volcanoclastic units. Spatially, rhyolite, andesite and associated pyroclastic rocks are most widespread. Overall, most Mesozoic volcanic rocks were coeval with the time of lithospheric thinning in the eastern part of the North China Craton [36]. Therefore, eastern CAOB constitutes an important area that records a significant Early Cretaceous giant igneous event in eastern China [37,38].

Several hypotheses have been proposed to interpret the tectonic setting of the Mesozoic volcanic and granitic rocks in the CAOB. Based on the supposed circular distribution of Mesozoic volcanic rocks within and around the CAOB, it was proposed that a mantle plume might have been responsible for the formation of such a huge area of volcanic and granitic rocks [39,40]. The second school of thought suggests that the Mesozoic volcanic rocks were formed due to subduction of the Mongol–Okhotsk Ocean and subsequent orogenic collapse [41,42].

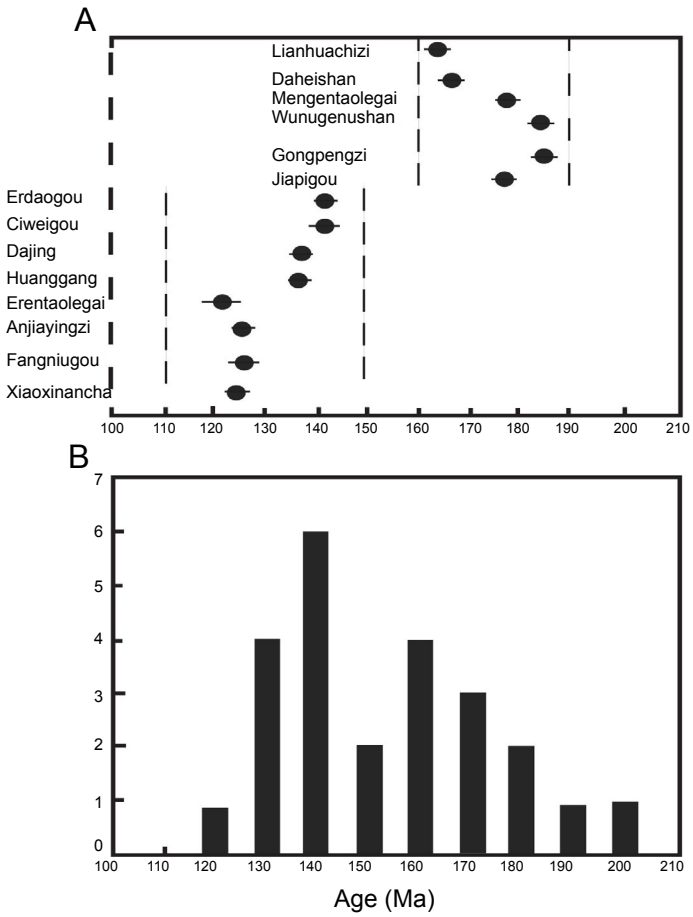


**Figure 7:** (A) Time span of base metal mineralization in the Central Asian Orogenic Belt. (B) Histogram of the magmatism in the Central Asian Orogenic Belt (the horizontal and vertical axes show the age and number of age data, respectively). Data are from [26-27] and this study.

A third model involves subduction of the Paleo-Pacific plate beneath eastern China [43,44].

Engebretson et al. proposed that the subduction directions of the Paleo-Pacific plate along the margin of eastern Eurasia changed during this interval [45]; for example, from NW-directed convergence from 180 to 145 Ma, to NNW-directed convergence from 145 to 85 Ma, and to west-directed convergence after 85 Ma. The belt of ~160 Ma plutons is aligned in a NE–SW direction perpendicular to the Palaeo-Pacific subduction direction, extending into the Central Asian Tectonic Zone to the north and the Yangtze Craton to the south, and shows evidence of NNE-striking thrusting [45]. This partial melting event can be best correlated with NW-directed subduction of the Palaeo-Pacific plate at 180–145 Ma [45]. Far to the west of the Western Block of the North China Craton, the north–south trend of the Western Ordos fold–thrust belt may also suggest a link with Palaeo-Pacific subduction along the eastern margin of Asia [46]. However, it is more likely to be a synthetic effect of eastward extrusion resulting from north–south compression between the northern and southern margins of the North China Craton and synchronous block faulting resulting from subduction of the Palaeo-Pacific plate. Because both the Yinshan–Yanshan orogen north of the North China Craton and the Qingling–Dabie orogen south of the North China Craton are synchronous with contraction from the Early and Middle Jurassic to Late Jurassic, two east–west-striking strike-slip faults in the northern and southern margins of the North China Craton cut across the fold–thrust belts [47].

Therefore we favor that the Daheishan porphyry Mo deposit was mainly formed during the transition period from the Paleo-Asian to Pacific domains. This is consistent with the termination of the CAOB and the onset of Pacific-plate accretion in the latest Triassic-Early Jurassic based on systematical U-Pb zircon ages and petrological studies on some gneisses and granitoids [6]. There was no solid evidence to show that any plume was responsible for these events so far and the Mongol-Okhotsk ocean is several hundreds of kilometers north of the study area. Therefore, the current study does not support the two alternatives although there could be possibly some joint contribution from them.

We further propose a slab melting model in which slab break-off may have continued by shallow subduction between adakite magmatism. Opening a slab window beneath the eastern CAOB could lead to multiple pulses of magmatism and production of crustal melts [48,49]. In light of the high transition metal contents of the Daheishan suite, elevated Cu contents are possible in these intrusive rocks. Such a hypothesis of the slab melting model can be more efficient in recycling the hydrothermal Cu-sulfides of the down going oceanic slab [50].

Based on these discussions, we propose that the widespread Mesozoic volcanic rocks in the CAOB region might have been generated in an extensional regime [47], but this extensional regime is mainly triggered by the subduction of the Paleo-Pacific plate in east China [45-47]

## Conclusions

The Daheishan porphyry Mo deposit is composed of quartz and sulfide stockwork and veinlets in the Daheishan granitoid. Hydrothermal alternation with potassic, propylitic, and phyllic assemblages are observed. Seven molybdenites yielded an isochron age of 168.0 ± 4.4Ma (2σ) with an initial 187Os of 0.08 ± 0.94 (MSWD=0.65), and model ages for individual analyses range between 165-172 Ma; The S isotopeic data support the hypothesis that a significant part of the metals and magmas have a mixed (crust + mantle) origin.

### Acknowledgement

We are indebted to, Mao, J.W., K.Z. Qin, Z .C., Zhang, Wang, Y.T., Zhang, L.C., Wang, Z. L. for discussions. Many of the ideas in this paper were initiated and rectified during these discussions. This study was financially supported by funds from the Chinese State 973 Project (2007CB411307), the Innovative Program of the Chinese Academy of Sciences (KZCX2-YW-Q04-08), the NSFC Project (40725009, 40421303, and 40572043), and Hong Kong RGC (7066/07P). This paper is a contribution to the ILP (ERAS) and IGCP 480.

### References

1. Wu FY, Jahn BM, Wilde S, Sun DY (2000) Phanerozoic continental crustal growth: Sr-Nd isotopic evidence from the granites in northeastern China. Tectonophysics 328: 87-113.
2. Wu FY, Wilde SA, Sun DY, Zhang GL (2004) Geochronology and petrogenesis of post-orogenic Cu, Ni-bearing mafic-ultramafic intrusions in Jilin, NE China. Journal of Asian Earth Science 23: 791-797.
3. Wu FY, Zhao GC, Sun DY, Wilde SA, Yang JH (2007) The Hulan Group: Its role in the evolution of the Central Asian Orogenic Belt of NE China. Journal of Asian Earth Science 30: 542-556.
4. Ge WC, Wu FY, Zhou CY, Zhang JH (2007) Porphyry Cu-Mo deposits in the eastern Xing'an-Mongolian Orogenic Belt: Mineralization ages and their geodynamic implications. Chinese Science Bulletin 52: 3416-3427.
5. Tang ZL, Qian ZZ, Ren BC, Zeng ZR., Wu JR, et al. (2005) Paleozoic Mineralization in China. Beijing: Geo1ogy Publishing House.
6. Wilde SA, Wu FY, Zhao GC, Zhou JB, Sklyarov E (2009) Termination of the eastern Central Asian Orogenic Belt due to onset of Pacific-plate accretion in the latest Triassic-Early Jurassic. International Field Excursion and Workshop on Tectonic Evolution and Crustal Structure of the Paleozoic Chinese Tianshan Urumqi, China.
7. Kravchinsky VA, Cogne JP, Harbert WP, Kuzmin MI (2002) Evolution of the Mongol-Okhotsk Ocean as constrained by new palaeomagnetic data from the Mongol-Okhotsk suture zone, Siberia. Geophysics Journal International 148: 34-57.
8. Zorin YA (1999) Geodynamics of the western part of the Mongolia-Okhotsk collisional belt, Trans-Baikal region (Russia) and Mongolia. Tectonophysics 306: 33-56.
9. Xiao WJ, Windley BF, Hao J, Zhai MG (2003) Accretion leading to collision and the Permian Solonker suture, Inner Mongolia, China: termination of the central Asian orogenic belt. Tectonics 22.
10. Wilde SA, Zhang XZ, Wu FY (2000) Extension of a newly identified 500 Ma metamorphic terrane in North East China: further U-Pb SHRIMP dating of the Mashan Complex, Heilongjiang Province, China. Tectonophysics 328: 115-130.
11. Lin W, Michel F, Sébastien N, Shang QH, Paul RR (2008) Permian-Triassic Amalgamation of Asia: insights from NE China sutures and their place in the final collision of North China and Siberia. CR Acad Sciences Paris 340: 190-201.
12. Xi AH, Gu LX, Li XJ, Ye SQ, Zhen YC (2005) Discussion on metallogenic epoch of Hongqiling Cu-Ni sulfide deposit, Jinlin Province. Mineral Deposits 24: 521-526.
13. Luo MJ, Zhang FM, Dong QY, Xu YR, Li SM, et al. (1991) China molybdenum deposits. Zhengzhou Henan Science and Technology Press.
14. Du AD, He HL, Yin NW, Zou X, Sun Y, Sun D et al, (1995) A study of the rhenium-osmium geochronometry of molybdenites. Acta Geologica Sinica 8: 171-181.
15. Du AD, Wang SX, Sun D, Zhao D, Liu D (2001) Precise Re-Os dating of molybdenite using Carius tube, NTIMS and ICPMS.
16. Shirey SB, Walker RJ (1995) Carius tube digestion for low-bank rhenium-osmium analysis. Analytical Chemistry 67: 2136-2141.
17. Stein HJ, Markey RJ, Morgan JW, Du AD, Sun YL (1997) Highly precise and accurate Re-Os ages for molybdenite from the East Qinling molybdenium belt, Shaanxi Province, China. Economic Geology 92: 827-835.
18. Stein HJ, Sundblad K, Markey RJ, Motuza G (1998) Re-Os ages for Archean molybdenite and pyrite, Kuittila-Kivisuo, Finland, and Proterozoic molybdenite, Kabeliai, Lithuania: testing the chronometer in a metamorphic and metasomatic setting. Mineralium Deposita 33: 329-345.
19. Markey R, Stein H, Morgan J (1998) Highly precise Re-Os dating for molybdenite using alkaline fusion and NTIMS. Talanta 45: 935-946.
20. Ludwig KR (2003) User's Manual for Isoplot 3.0: A Geochronological Toolkit for Microsoft Excel. Berkeley Geochronology Center Special Publication 4.
21. Mao JW, Zhang ZC, Zhang ZH, Du AD (1999) Re-Os isotopic dating of molybdenites in the Xiaoliugou W (Mo) deposit in the northern Qinling mountains and its geological significance. Geochimica et Cosmochimica Acta 36: 1815-1818.
22. Stein HJ, Markey RJ, Morgan JW, Hannah JL, Schersten A (2001) The remarkable Re-Os chronometer in molybdenite: how and why it works. Terra Nova 13: 479-486.
23. Selby D, Creaser RA (2001) Re-Os geochronology and systematics in molybdenite from the Endako porphyry molybdenum deposit, British Columbia, Canada. Economic Geology 96: 197-204.
24. Berzin NA, Sotnikov VI, Economou EM, Eliopoulos DG (2005) Distribution of rhenium in molybdenite from porphyry Cu-Mo and Mo-Cu deposits of Russia (Siberia) and Mongolia. Ore Geology Reviews 26: 91-113.
25. Huang DH, Du AD, Wu CY, Liu LS, Sun YL et al, (1996) Geochronology of molybdenum (copper) deposits in the north China platform: Re-Os age of molybdenite and its geological significance. Mineral Deposits 15: 289-297.
26. Ohmoto H, Goldhaber MB (1997) Sulfur and carbon isotopes. In: Barnes, HL (Ed.), Geochemistry of hydrothermal Ore deposits, 3rd ed, John Wiley and Sons, New York.
27. Mao JW, Xie GQ, Zhang ZH, Li XF, Wang YT, et al, (2005) Mesozoic large-scale metallogenic pulses in North China and corresponding geodynamic settings. Acta Petrologica Sinica 21:169-188.
28. Mao JW, Wang YT, Lehmann B, Yu JJ, Du AD, et al, (2006) Molybdenite Re–Os and albite $^{40}Ar/^{39}Ar$ dating of Cu–Au–Mo and magnetite porphyry systems in the Yangtze River valley and metallogenic implications. Ore Geology Reviews 29: 307-324.
29. Mao JW, Xie GQ, Bierlein F, Qu WJ, Du AD, et al, (2008) Tectonic implications from Re–Os dating of Mesozoic molybdenum deposits in the East Qinling–Dabie orogenic belt. Geochimica et Cosmochimica Acta 72: 4607-4626.
30. Lin Q, Ge WC, Wu FY, Sun DY, Cao L (2004) Geochemistry of Mesozoic granites in Da Hinggan Ling ranges. Acta Petrologica Sinica 20, 403-412.
31. Ge WC, Wu FY, Zhou CY, Zhang JH (2005) Zircon U-Pb ages and its significance of the Mesozoic granites in the Wulanhaote Region, central Great Xing'an Range. Acta Petrologica Sinica 21: 749-762.
32. Zhang JH, Ge WC, Wu FY, Wilde SA, Yang JH, et al, (2008) Large-scale Early Cretaceous volcanic events in the northern Great Xing'an Range, Northeastern China. Lithos 102: 138-157.
33. Jahn BM, Wu FY, Chen B (2000) Massive granitoid generation in central Asia: Nd isotopic evidence and implication for continental growth in the Phanerozoic. Episodes 23: 82-92.
34. Wu FY, Sun DY, Li HM, Jahn BM, Wilde SA (2002) A-type granites in northeastern China: age and geochemical constraints on their petrogenesis. Chemical Geology 187: 143-173.
35. Song J, Dou L (1997) Mesozoic-Cenozoic Tectonics of Petroliferous Basins in Eastern China and their Petroleum Systems. Petroleum Industry Press, Beijing.
36. Wu FY, Sun DY (1999) Mesozoic magmatism and lithospheric thinning in the eastern China. Journal of Changchun Science and Technology University 29:313-318.
37. Wu FY, Lin JQ, Wilde SA, Sun DY, Yang JH (2005) Nature and significance of the Early Cretaceous giant igneous event in eastern China. Earth and Planetary Science Letters 233: 103-119.

38. Wang F, Zhou XH, Zhang LC, Ying JF, Zhang YT, et al, (2006) Late Mesozoic volcanism in the Great Xing'an Range (NE China): timing and implications for the dynamic setting of NE Asia. Earth and Planetary Science Letters 251: 179-198.

39. Shao JA, Zang SX, Mou BL (1994) Extensional tectonics and asthenospheric upwelling in the orogenic belt: a case study from Hinggan–Mongolia Orogenic belt. Chinese Science Bulletin 39: 533-537.

40. Shao JA, Li XH, Zhang LQ, Mu BL, Liu YL (2001a) Geochemical conditions for genetic mechanism of the Mesozoic bimodal dyke swarms in Nankou-Guyaju. Geochemica 30: 517-524.

41. Fan WM, Guo F, Wang YJ, Lin G (2003) Late Mesozoic calc-alkaline volcanism of post-orogenic extension in the northern Da Hinggan Mountains, Northeastern China. Journal Volcanology Geothermal Research 121: 115-135.

42. Meng QR (2003) What drove late Mesozoic extension of the northern China–Mongolia tract? Tectonophysics 369: 155-174.

43. Zhu G, Wang YS, Liu GS, Niu ML, Xie CL, et al, (2005) $^{40}Ar/^{39}Ar$ dating of strike-slip motion on the Tan-Lu fault zone, East China. Journal of Structure Geology 27: 1379-1398.

44. Sun WD, Li SG, Chen YD, Li XH (2007) The golden transformation of the Cretaceous plate subduction in the west Pacific. Earth and Planetary Science Letters 262: 533-542.

45. Engebretson DC, Cox A, Gordon RG (1985) Relative motions between oceanic and continental plates in the Pacific basin. Geological Society of America 206: 1-59.

46. Darby BJ, Rifts BD (2002) Mesozoic contractional deformation in the middle of the Asian tectonic collage: the intraplate Western Ordos fold–thrust belt, China. Earth and Planetary Science Letters 205: 13-24.

47. Li SZ, Kusky TM, Zhao GC, Wu FY, Liu JZ, et al, (2007) Mesozoic tectonics in the Eastern Block of the North China Craton: implications for subduction of the Pacific plate beneath the Eurasian plate. Geological Society, London 280.

48. Thorkelson DJ, Taylor RP (1989) Cordillera slab window. Geology 17: 833-836.

49. Percival JA, Stern AA, Rayner N (2003) Archean adakite from the Ashunipi complex, eastern Superior Province, Canada: geochemistry, geochronology and tectonic significance. Contributions to Mineralogy and Petrology 145: 265-280.

50. Han CM, Xiao WJ, Zhao GC, Mao JW, Yang JM, et al, (2006) Geological characteristics and genesis of the Tuwu porphyry copper deposit, Hami, Xinjiang, Central Asia. Ore Geology Reviews 29: 77-94.

51. Smoliar ML, Walker RJ, Morgan JW (1996) Re-Os ages of group IIA, IIIA, IVA and VIB iron meteorites. Science 271: 1099-1102.